Fast physically accurate rendering of multimodal signatures of distributed fracture in heterogeneous materials

Yon Visell, *Member, IEEE*

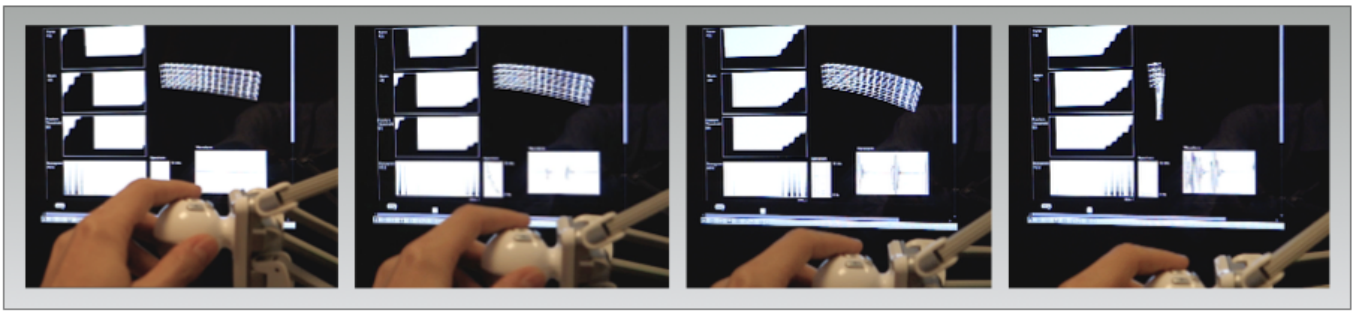

Fig. 1. Fast, interactive rendering of fracture in heterogeneous materials.

Abstract— This paper proposes a fast, physically accurate method for synthesizing multimodal, acoustic and haptic, signatures of distributed fracture in quasi-brittle heterogeneous materials, such as wood, granular media, or other fiber composites. Fracture processes in these materials are challenging to simulate with existing methods, due to the prevalence of large numbers of disordered, quasi-random spatial degrees of freedom, representing the complex physical state of a sample over the geometric volume of interest. Here, I develop an algorithm for simulating such processes, building on a class of statistical lattice models of fracture that have been widely investigated in the physics literature. This algorithm is enabled through a recently published mathematical construction based on the inverse transform method of random number sampling. It yields a purely time domain stochastic jump process representing stress fluctuations in the medium. The latter can be readily extended by a mean field approximation that captures the averaged constitutive (stress-strain) behavior of the material. Numerical simulations and interactive examples demonstrate the ability of these algorithms to generate physically plausible acoustic and haptic signatures of fracture in complex, natural materials interactively at audio sampling rates.

Index Terms—Physical simulation, multimodal rendering, virtual reality

1 Introduction

It has been a longstanding goal in virtual reality and computer animation to simulate the interactive, multimodal behavior of natural objects and surroundings in plausibly realistic ways. However, the mechanics of many common interactions and materials are highly complex. For example, when subjected to sufficiently large stresses, a diverse variety of natural media, ranging from wood to gravel, give rise to quasi-random, fracture-like processes yielding fast and unpredictable force fluctuations [31, 10, 41, 6, 43, 28, 42, 30]. Some of these include fracture in natural fiber composites [14, 2, 1] and stress fluctuations during shear sliding on granular media [4, 8, 34, 33]. Such processes have attracted interest in scientific and engineering research because of the unusual variety of phenomena they exhibit, and because of their relevance to many natural materials and physical interactions [14, 2]. A full account of the physics of these processes remains elusive, due to the microscopically disordered nature of the materials and their large number of constituent elements. Nonetheless, some of the most salient aspects of their behavior have been revealed in statistical physics analyses undertaken during the last few decades [2, 14, 31].

A basic problem is to predict the macroscopic patterns of failure from micromechanical properties, and to simulate their behavior without explicitly integrating the full micromechanical state, which is often computationally prohibitive. Stress distributions in granular media also share many common features with fiber composites. Remarkably, both material categories can be considered to bear stress predominantly along arrays of brittle, one-dimensional structures with randomly distributed strengths. In prior literature, as in the present contribution, this has been exploited to facilitate both analysis and modeling.

• *Author is with Drexel University. E-mail: yon.visell@drexel.edu.*

Manuscript received 18 September 2014; accepted 10 January 2015; posted online 23 March 2014; mailed on 1 May 2014.
For information on obtaining reprints of this article, please send e-mail to: tvcg@computer.org.

Rendering brittle fracture in heterogeneous materials

Methods for the computational rendering and animation of fracture-like processes have advanced in recent decades. The notion of simulating material deformation, fracture, and related phenomena was introduced by Terzopoulos [47]. Numerous subsequent studies have introduced different methods of fracture rendering [20, 35, 36, 39, 49, 32, 45, 49, 12, 27, 29]. A review would be beyond the scope of the present contribution. Fewer studies have investigated rendering fracture in microscopically heterogeneous materials, such as wood. To date, those that have done so are based on physically inaccurate heuristics [38], or have been otherwise impractical for rendering damage in macroscopically large samples, due to the high density of constituent elements involved [46]. In contrast, the methods we introduce here are strongly grounded in the relevant physics, and can efficiently render fracture in large ensembles of fibers in real time.

Particle-based rendering methods have been used to animate granular media [5, 50, 25]. However, known algorithms are unable to capture the characteristic spatial and temporal stress fluctuations that are observed in real granular materials [14]. Multimodal (haptic and/or auditory) rendering of such phenomena is even more prohibitive, due to the high sampling rates that are required for perceptual fidelity, for

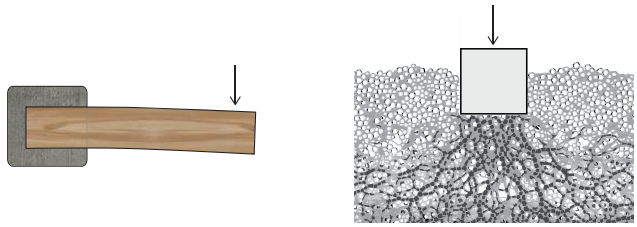

Fig. 2. Fiber bundle models, the foundation of the present work, have been successfully used to model brittle fracture in materials that effectively bear stress along arrays of one-dimensional structures loaded in parallel. Examples include fiber composites such as wood (left), and granular media, such as sand or gravel (right).

stable, artifact-free rendering [26], and due to the rapid temporal fluctuations involved.

The mechanics of quasi-brittle, heterogeneous materials is complicated by the predominance of highly disordered micromechanical structures, which lead to large random spatial and temporal stress fluctuations. Physically accurate simulation of such materials has generally only been possible using numerically intensive methods from material science and physics [14, 2, 31], where lattice models with large numbers of spatial degrees of freedom predominate. These models are computationally costly, but phenomenologically accurate.

The present contribution is enabled through recent work in the statistical physics of fracture [3]. It identified a purely temporal fracture process, reviewed below, which captures the stochastic temporal dynamics without representing spatial degrees of freedom. In that work, we identified a stochastic jump process exactly capturing the fluctuating pattern of failure in a fiber bundle model of fracture and obtained a factorization, separating out a mean constitutive response that closely matches the nonlinear stress-strain behavior of the exact model. The latter aspect allowed the (smooth) stress-strain dynamics to be simulated deterministically, without tracking the (rapidly fluctuating) random failure history in the material. The former provides an iterative stochastic description of instants of failure in the material as it is loaded. The work presented here makes use, and builds upon, both innovations in order to enable real-time rendering of interactions with these complex materials.

Summary of Contributions and Content

The main contributions of the present paper are:

1. A novel algorithm for the efficient, real-time rendering of multimodal signatures of fracture in natural and man-made fiber composite materials, based on a statistical model of fracture developed by the author [3].

2. A derivation of a stochastic point process model of strained or shear granular media, based on the inverse Fiber Bundle Model. This construction is inspired by the aforementioned one, and is presented here for the first time.

3. An algorithm for fast multimodal rendering of fracture-like processes that arise in strained or sheared granular media.

4. Novel applications of the foregoing algorithms to the interactive, multimodal rendering of fracture in fiber composite materials. Interactions are enabled by a force-feedback device and (in the case of audio) a loudspeaker.

Efficiency is guaranteed by a construction which allows a distributed physical medium to be modeled as a lumped-parameter point process, as in item (1.) above. This, in turn, effectively reduces the rendering computations to the integration of a 2nd-order dynamical (nonlinear) dynamical system coupled with a sequential random number sampling procedure. For this reason, most of the material below is devoted to exposition of this method and its application to the material simulations of interest. Further details are provided in a separate publication of the authors [3].

The organization of the remainder of this paper is as follows. The next section provides a brief review of a well studied lattice statistical physical model of fracture processes, the Fiber Bundle Model, that has been found to capture the salient physical phenomena in materials and processes like those mentioned above. Then, we present the construction of a low-dimensional stochastic process that exactly captures the behavior of the aforementioned model in the limit of long-range load transfer, as demonstrated theoretically and numerically.

2 Fiber Bundle Model of Material Fracture

Fiber Bundle Models (FBMs) are lattice statistical physical models of fracture for failure processes in quasi-brittle, heterogeneous materials [2, 40]. Fracture processes in these materials unfold in unpredictable ways, particularly when compared with fracture in homogeneous solid materials. They are accompanied by a host of distinctive phenomena that have been documented in prior literature, including statistical strength distributions, stress fluctuations, reorganization accompanying failure, acoustic emissions, and accumulated damage. These phenomena, while highly salient, are not well captured by deterministic continuum mechanics models of fracture, which has led to the development of statistical approaches, including the FBM.

These models consist of lattices of N parallel elastic or viscoelastic fibers each sharing a quantity σ_i, $i = 1,2,\ldots,N$, of the force, F, on the bundle (Figure 3). The strain $x_i(t)$ of each ith fiber is governed by the physical equation

$$F(t) = \sum_{i=1}^{N} \sigma_i(t) = \sum_{i=1}^{N} \left(\phi_i \sigma_i^F(t) + \sigma_i^R(t) \right). \tag{1}$$

The strain-dependent, per-fiber load is $\sigma_i = \sigma_i(x_i, \dot{x}_i, \ddot{x}_i, \cdots)$. It may be expressed in terms of a part σ_i^F born by intact fibers (for which the indicator variable $\phi_i = 1$) and another, σ_i^R, that is born by the surrounding (non-fibrous) material matrix, which persists after failure ($\phi_i = 0$). A minimal micromechanical model for viscoelastic and plastic effects (Fig. 3, modified Kelvin-Vogt model) may be given as follows:

$$\sigma_i^F(t) = (b_F \dot{x}_i + k_F x_i),\ \sigma_i^R = (b_R \dot{x}_i + m \ddot{x}_i) \tag{2}$$

The dynamical equation depends upon an effective (per-fiber) mass coefficient m (proportional to the effective fiber mass), elastic constant k_F and damping constants b_F and b_R representing the pre- and post-failure relaxation of the fiber. [17]. A number of variations of this micromechanical model are possible [40].Fibers fracture when $x_i(t)$ exceeds a fiber-specific breaking threshold ξ. The thresholds are random variables, with $\xi \sim p(\xi)$, where $p(\xi)$ is a random distribution of fiber strengths. After fracture, the load is redistributed among those that survive. A common simplifying assumption (Equal Load Sharing, ELS) is that upon the failure of an individual fiber its load is equally distributed, so that the load on each intact fiber depends on the total load and number N_F of intact fibers $\sigma_i = F/N_F$. We adopt this assumption here, and discuss extensions to local load sharing in Sec. 5, below.

Each fracture event decreases the number $N_F(t)$ of intact fibers at time t, increasing the load on surviving fibers, and cascading in further failures. This continues until $x(t) < \xi^*$, where ξ^* is the threshold of the weakest surviving fiber. When a critical value F_c of the applied stress is reached, the bundle is incapable of supporting the redistributed load, and all remaining fibers break. The number N_F of fibers surviving at a given load thus depends on the load history and random assignment of thresholds.

Disorder in this model can be introduced through the initial assignment of random fiber thresholds, which model the random strengths of micromechanical elements in the medium. These thresholds can be viewed as random initial conditions, with the subsequent evolution occurring deterministically. Instead, we can regard the sequence of

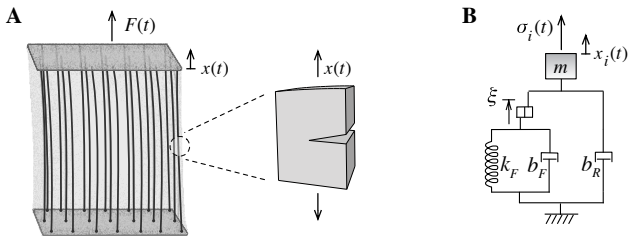

Fig. 3. Illustration of the fiber Bundle Model of fracture. **A.** A lattice of N viscoelastic-plastic fibers is loaded with external force $F(t)$. The weakest surviving fiber strains under local stress σ_i. **B.** A mechanical analog in the form of a modified Kelvin-Vogt element. The plastic element fails when the force on it is greater than a random threshold ξ, a disconnecting spring k_F and damper b_F. Post-fracture relaxation is modeled via a persistent damping factor, b_R.

failure points as a random point process whereby the threshold ξ representing the weakest fiber jumps in value at the time of each fracture. In the next section, we provide an explicit formulation of the this process.

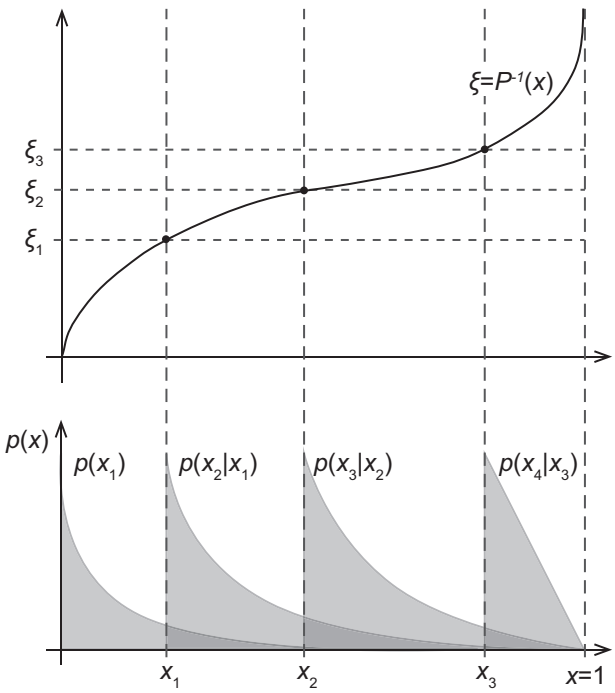

Fig. 4. The sequential sampling algorithm described in Eq. (**??-??**). The next value ξ_j of the threshold is determined from s_{j-1}, with the distribution represented by the shaded area to the right of s_j, and the number of remaining fibers, $N_{F,j}$. $\xi(t)$ is sampled in a way that depends on its value $\xi(t-dt)$ at the preceding instant and the load history, $\sigma(\tau), \tau \leq t$. The process is non-Markovian, because the kth such distribution depends on the number $N-k-1$ of preceding fractures.

3 Time-Domain Stochastic Process Formulation

The two key variables reflecting the instantaneous state of this model are the number N_F of intact fibers and the breaking threshold ξ^* of the weakest intact fiber. At the instant of failure, ξ^* increases by a random amount Δ that is related to $p(\xi)$ and the number N_F of surviving fibers. The result is a stochastic jump process for a temporally fluctuating threshold $\xi(t)$, equal at any instant t to ξ^*, whose jth piecewise constant value $\xi(t) = \xi_j$ is reached at the instant $\xi(t-dt) = \xi_{j-1}$ is surpassed. One can interpret the failure series as a sequential, monotonically increasing random process that reproduces the specified strength distribution $p(\xi)$. A temporally local definition of the process $\xi(t)$ that conforms to the desired strength distribution $p(\xi)$ may obtained by sequentially sampling failure thresholds, rather than integrating the dynamical state of the lattice of all fibers. This can be done using a method derived from the inverse transform sampling technique of random number generation [9]; we briefly review the method, which is presented for the first time in a separate work of the author [3]. Let $P(\cdot)$ be the cumulative distribution function of $p(\xi)$, and let $N_{F,j} = N - j + 1$ is the number of surviving fibers prior to the jth failure. Denote by $\xi(t) = \xi_j$, where ξ_j represents the strength of the weakest surviving fiber at time t. When a fracture event occurs, $\xi(t)$ jumps in value and the number of surviving fibers, $N_F(t)$, decreases for each failed fiber. This happens whenever the dynamic strain $x(t)$ exceeds $\xi(t)$. A fracture event at time t yields a jump from ξ to a new value ξ' given by

$$s' = s + (1-s)\left(1 - u^{1/N_F(t)}\right), \tag{3}$$

$$\xi' = P^{-1}(s'). \tag{4}$$

Upon substituting and using $\xi' = P^{-1}(s')$, this provides a simple iterative expression for the fracture event:

$$\xi' = P^{-1}\left(P(\xi) + \left(1 - P(\xi)\right)\left(1 - u^{1/N_F(t)}\right)\right). \tag{5}$$

The resulting sequence ξ_j is equivalent to a set of N independent samples from $p(\xi)$ sorted in increasing magnitude.

The fracture size at time t depends on the state of the co-evolving random process $N_F(t)$ and on the value of the strength $\xi(t)$ prior to failure. The fracture time depends on the values of $\xi(t)$ and the strain $x(t)$. This algorithm reproduces the ensemble of samples from $p(\cdot)$ by sequentially sampling the conditional distributions $p(\xi_j \,|\, \xi_{j-1}, N_{F,j})$, as in Eq. (5); see Fig 4. The resulting process is non-Markovian, because it depends on the sample history through $N_F(t)$, and through the dynamical stress-strain equation (1).

Mean damage approximation: In the foregoing construction, the global strain threshold $\xi(t)$ depends on the random level of damage at the time of fracture (represented by $N - N_F$), which depends on the history of the sample. This section describes an effective model with smooth constitutive behavior, facilitating efficient simulation.

The instantaneous strain $x(t)$ depends on the stochastic evolution of damage in the lattice. However, the real dynamics will tend to average over the fluctuations in stress. This suggests a modeling approach that averages over fluctuations to approximate the nonlinear strain evolution deterministically, with random effects captured by the variable ξ. One can achieve this by replacing $N_F(t)$, where it appears in the threshold and evolution equations (5) and (1), by the expected survival number $\overline{N}_F(t)$ given the load history. Under ELS, its value is $\overline{N}_F = N(1 - P(x))$, with x the maximum strain achieved during loading. $\overline{N}_F$ is the mean damage that would be expected for an ensemble of instances of the model subjected to the given load history.

The expected survival number $\overline{N}_F(t)$ depends on the strain via

$$\overline{N}_F(t) = N\left(1 - P(x^*(t))\right), \quad x^*(t) = \max_{t'<t} x(t'). \tag{6}$$

Under monotonically increasing loading, this equals $\overline{N}_F(t) = N(1 - P(x(t)))$. Upon replacing N_F by $\overline{N}_F$ one can factorize the model into a deterministic part governing the nonlinear stress-strain response,

$$F(t) = \overline{N}_F(t)\sigma^F(t) + N\sigma^R(t) \tag{7}$$

and a stochastic process describing the stress fluctuations:

$$\xi' = P^{-1}\left(P(\xi) + \left(1 - P(\xi)\right)\left(1 - u^{1/\overline{N}_F}\right)\right) \tag{8}$$

$$\text{while } x(t) > \xi. \tag{9}$$

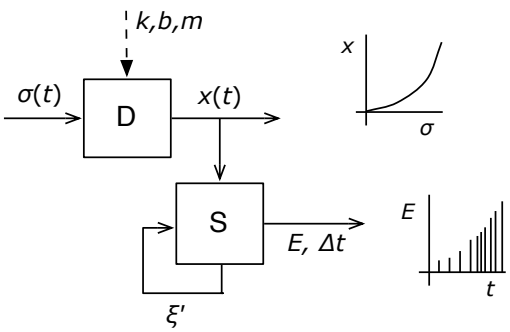

Fig. 5. The mean damage model $\overline{M}$ is composed of a deterministic process D describing the mean constitutive response and a stochastic process S describing the fluctuations.

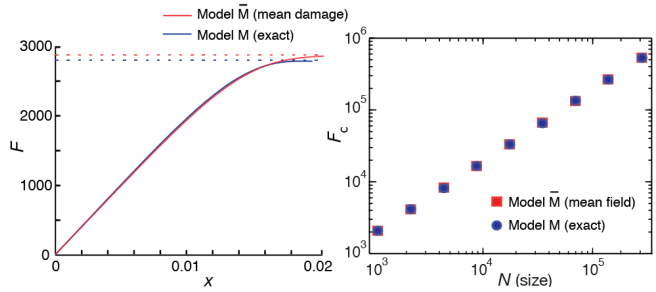

Fig. 6. Left: The empirical stress-strain behavior of models M and $\overline{M}$. Both were obtained under quasistatic loading, at supra-critical values of the maximum stress, $F > F_c$, computed from 200 uniformly distributed values of the terminal load, using simulations with 2000 fibers. Dashed blue line: critical stress values of $F_c(M) = 2800, F_c(\overline{M}) = 2850$. Dashed red lines: 95% confidence intervals. Right: Critical stress values obtained from the same simulations. Results from the study [3].

For now, refer to the original FBM model as M and the approximation obtained through this "mean damage" replacement as $\overline{M}$. The latter takes on explicit form when a fiber strength distribution $p(\xi)$ is specified.

3.1 Statistical Distributions $p(\xi)$ of Fiber Breaking Thresholds

Uniform fiber strength distribution: In one commonly used fiber strength distribution, $p(\xi)$ is assumed to be uniformly distributed on the unit interval $[0,1]$. Assuming a minimal Kelvin-Vogt type viscoelastic micromechanical model, the homogenized nonlinear stress-strain response becomes:

$$F(t) = N(1-x)\,(b_F\dot{x} + k_F x) + N(b_R\dot{x} + m\ddot{x}) \tag{10}$$

while the failure event is described by sampling ξ' as:

$$\xi' = \xi + (\xi - 1)(u^{1/(N(1-\xi))} - 1) \tag{11}$$

with u taken to be a sample of a random variable uniformly distributed in $[0,1]$.

Weibull fiber strength distribution: The Weibull function is frequently used as a statistical distribution for solid strength in materials science [48]. The Weibull CDF can be written

$$P(\xi) = 1 - \exp(-\xi/\lambda)^k \Theta(\xi). \tag{12}$$

Here λ and k are scale and shape parameters, and $\Theta(\cdot)$ is the Heaviside step function, with $\Theta(\xi) = 0$ for $\xi < 0$ and $\Theta(\xi) = 1$ for $\xi > 0$. The constitutive model is

$$\sigma(t) = N\exp\{(-x/\lambda)^k\}\,(b_F\dot{x} + k_F x) + N(b_R\dot{x} + m\ddot{x}) \tag{13}$$

and the fracture event is sampled as

$$\xi' = \lambda\left(\frac{\xi}{\lambda}\right)^k \log\left(1 - e^{(-\xi/\lambda)^k}\left(1 - u^{1/(N\exp\{(-\xi/\lambda)^k\})}\right)\right)^{1/k} \tag{14}$$

Constitutive behavior and fluctuations: The value of the critical stress F_c and distributions of fluctuations as failure approaches are known to depend weakly on the precise distribution of fiber strengths [2, 40]. Specifically, the constitutive evolution of $\overline{M}$ differs from that of M due to fluctuations in the survival number N_F about its mean. This can be regarded as a source of high-frequency noise that should approximately integrate to zero, so we reasoned that even if these fluctuations are significant, the model $\overline{M}$ would yield similar behavior to M. Indeed, this turns out to be the case; detailed numerical comparisons are provided in a separate publication. Simulation runs are qualitatively indistinguishable for both models. Figure 7 provides representative results (samples of model M), and a comparison of constitutive behavior and failure thresholds for both models is given in 6. In these simulations, the per-fiber load increases linearly until the current threshold level $\xi(t)$ is met, at which point one or more fibers fail and a new value of $\xi(t)$ is sampled. The size and density of these failure events increase with the applied load, until the model reaches a stable point, or a critical load is achieved, causing the bundle to collapse.

Stress-strain relationships and critical load estimates are compared for both models in Figure 6. Qualitatively and quantitatively, both are nearly identical, with an error of less than 2% in the critical load F_c for all bundle sizes examined (size $N = 1000$ to 256000), indicating that the mean macroscopic behavior of the model is well-preserved by the approximation.

Figure **??** provides evidence that this construction preserves the most salient physical phenomena captured by the FBM. It shows that the empirical distributions of failure event time intervals dt and of energy fluctuations dE exhibit power-law scaling with exponents consistent with prior literature [13, 40, 22],

4 Stress Fluctuations in Compressed Granular Media: Inverse Fiber Bundle Model

Complex patterns of force fluctuations accompany the compression of stiff granular materials, which, as in the case of fiber composite materials, have been successfully modeled in terms of the inelastic failure of one-dimensional structures loaded in parallel [15, 18]. The latter arise due to the organization of stress in granular materials in highly heterogeneous force networks, in the form of force chains percolating prevailingly along the direction of the principle axis of stress. These chains are created and restructured due to relative displacements of the grains, which rearrange their positions until a stronger, stable configuration is reached. Energy is rapidly dissipated in granular assemblies, and hence these rearrangements occur rapidly and highly inelastically, giving rise to large transient stress fluctuations that provide valuable information about the evolution of force chains during loading [23, 15].

4.1 Inverse FBM

A model for the evolution of force chains during compression was proposed by Hidalgo et al. [15, 18], as an extension of the continuous damage Fiber Bundle Model [24, 16]. In experiments on ensembles of granular particles, the model was able to effectively capture both nonlinear constitutive behavior of the medium and predicted the amplitude distribution of acoustic signals emitted by microscopic rearrangements of the particles during compression.

In this model, granular force chains are represented by an array of fibers loaded in parallel with randomly distributed failure thresholds. However, in contrast to the standard FBM, chains restructure after failure, becoming multiplicatively stronger and stiffer. If k is the pre-failure effective stiffness, and k' is the value after failure, then

$$k' = ak = k(1+\alpha), \quad \alpha > 0. \tag{15}$$

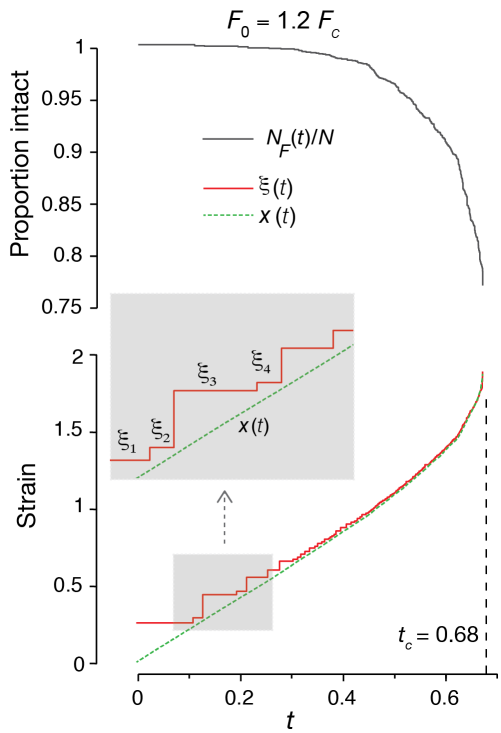

Fig. 7. Response to a linear ramp load, $F(t) = F_0 r(t)$, where $r(t) = t/\tau_0$ for $0 \le t \le \tau_0 = 0.8$. $N = 2000$ fibers, and Weibull-distributed thresholds (parameters $k = 4$ and $\lambda = 2.5$). Top row: Survival fraction $N_F(t)/N$ vs t. Maximum stress, F_0, is shown relative to critica l stress, $F_c \approx 2800$. Here, $F_0 = 1.2F_c$. Failure occurs at $t = 0.68$. Bottom row: Threshold $\xi(t)$ and strain $x(t)$ vs t.

For this reason, it has been called the inverse Fiber Bundle Model.

The bundle grows progressively stronger, rather than weaker (as in the FBM), corresponding to an increase in packing density of the medium. The constitutive dynamics of the bundle can be described, using the parametrization of Section 3, by

$$\sigma(t) = A(t)(b_F\dot{x} + k_F x), \sigma(t) = (N + \alpha I_F)(b_F\dot{x} + k_F x) \tag{16}$$

where

$$A(t) = \sum_{j=1}^{N} (1+\alpha)^{n_j(t)}, \tag{17}$$

$$K = k_F \sum_{j=1}^{N} (1+\alpha)^{n_j} \tag{18}$$

and $n_j(t)$ is the number of failures of the jth fiber at time t. Here, it is assumed that the damping ratio is preserved during evolution, so that $b' = b(1+\alpha)$.

When a given fiber has failed a maximum number $n_{\max}$ of times ($n_{\max}$ is a parameter of the model), it is assumed to be unable to further restructure, attaining a maximum stiffness of $k_{\max} = k_F(1+\alpha)^{n_{\max}}$. Subsequently, that fiber contributes a linear response. When all fibers have failed $n_{\max}$ times, the bundle enters a linear response regime.

4.2 IFBM: Time-domain stochastic process formulation

Although the inverse FBM is amenable to theoretical analysis, the present contribution focuses on applying an analogous modeling and simulation method to that of Section 3. The value of α, the relative increase in stiffness at each fracture, can generally be assumed to be

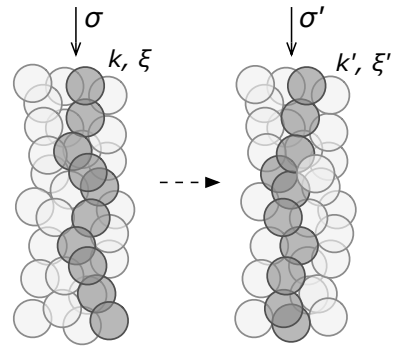

Fig. 8. Compression results in rapid events through which granular force chains become stronger, stiffer and straighter.

small (in the simulations below, $\alpha = 0.005$). Thus, one can approximate

$$A(t) \approx \sum_{j=1}^{N} (1 + \alpha n_j(t)) = N + \alpha I_F(t), \tag{19}$$

where $I_F(t)$ is the total number of failure events until time t.

The breaking threshold of a fiber increases upon failure. Thus, because all threshold are assumed to be drawn from the same distribution, the sequential algorithm of Section 3 can be used for simulation. After a failure, the next lowest threshold of the model is drawn according to

$$\xi' = P^{-1}\left(P(\xi) + \left(1 - P(\xi)\right)\left(1 - u^{1/N_T}\right)\right). \tag{20}$$

In the mean damage approximation, the discrete random variables $I_F(t)$ and $N_T(t)$ appearing in (16) and (20) may plausibly be replaced by their expected values, based on arguments similar to those used in the foregoing, yielding

$$\sigma(t) = (N + \alpha \bar{I}_F(t))(b_F\dot{x}(t) + k_F x(t)). \tag{21}$$

The expected number of failures $\bar{I}_F(t)$ at a given strain level is given by

$$\bar{I}_F(t) = n_{\max} N P(x^*(t)), \quad x^*(t) = \max_{t'<t} x(t'). \tag{22}$$

The expected survival number is, as for the Fiber Bundle Model, given by $\bar{N}_F(t) = N(1 - P(x^*(t)))$. Finally, the expected value of the number of remaining failures in the bundle is $\bar{N}_T = \bar{N}_F n_{\max}$. The constitutive and fluctuating response of this model can be written as

$$\sigma(t) = N(1 + \alpha n_{\max} P(x^*))(b_F\dot{x} + k_F x). \tag{23}$$

and

$$\xi' = P^{-1}\left(P(\xi) + \left(1 - P(\xi)\right)\left(1 - u^{[N n_{\max}(1 - P(x^*))]^{-1}}\right)\right) \tag{24}$$

Failure criteria For a material sample under a uniform, uniaxial load, either a maximum stress or maximum strain criterion may be used (the latter being identical to that employed for the fiber composite model of Section 3). In a local model of failure in a three-dimensional volume of granular material, the breaking threshold depends on the magnitude and directions of stresses or strains, because the load bearing force chains in the material reorganize to align with the direction of maximum stress. For coarse-grained soils or other granular media, failure can often be described by a Mohr-Coulomb yield criterion. This can be written as

$$s/n = \tan(\phi), \tag{25}$$

where s/n is the ratio of maximum and minimum principle stresses at the location of interest, and the parameter ϕ, the angle of repose (or angle of internal friction) of the granular material, describes the material strength.

4.3 Numerical validation

The mean damage inverse Fiber Bundle Model presented above was simulated under uniaxial, stress-controlled loading, in the same manner as in Section 3.1. A Weibull distribution of breaking thresholds was used with the same values of the parameters as used in the previous simulations. Figure 9 shows typical response profiles of the model under ramp loading conditions. As noted above, the nonlinear stress-strain relation is, opposite to the case of the Fiber Bundle Model, concave, corresponding to the increasing stiffness of the granular medium as it is compressed.

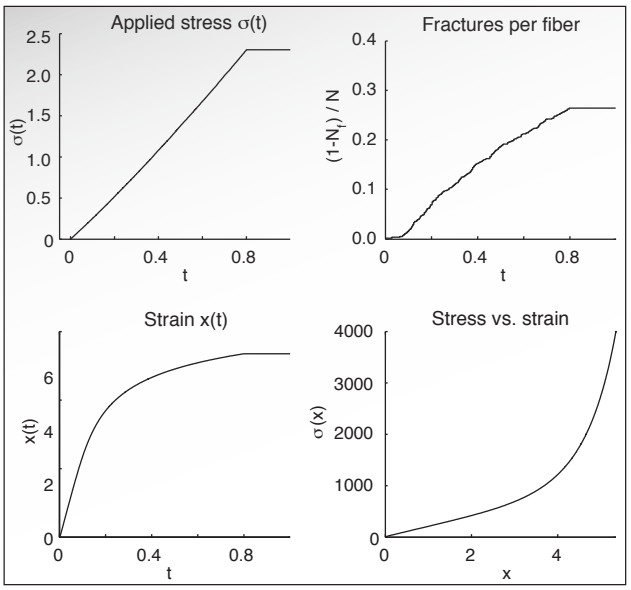

Fig. 9. Response of the inverse Fiber Bundle Model under ramp loading conditions. Top Left: Applied stress vs time. Top Right: Number of fracture events per fiber vs time. Bottom Left: Strain $x(t)$. Bottom right: Constitutive, stress-strain behavior. Data shown is based on 200 simulations of bundles with 2000 fibers subjected to ramp loading with maximum stress $\sigma = 2667$. Other simulation parametesr were as given in Figure 7.

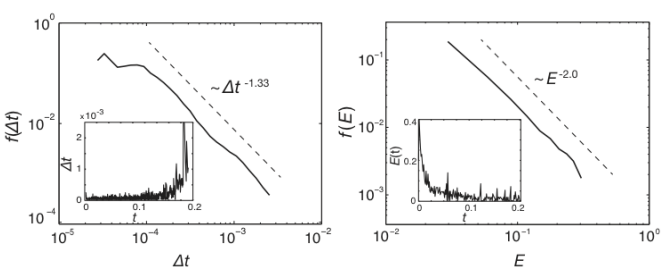

Fig. 10. Left: Empirical distribution of times between failure events, Δt, for the inverse Fiber Bundle Model. Right: Distribution of failure energy fluctuations (computed in windows of duration 0.005), exhibiting power-law scaling over more than one order of magnitude. Inset: Energy fluctuation size vs time during one simulation trial. Distributions were computed from 500 simulations of bundles with 2000 fibers subjected to ramp loading with maximum stress $\sigma_0 = 10^5$ and $n_{\max} = 20$. Other simulation details were as given in Figure 7.

Figure 10 presents empirical distributions of the times Δt between failure events and of the energy fluctuations of the model during loading. Both were computed as in Section 3.1. Energy fluctuations are observed, for large enough values of $n_{\max}$, to scale as $p(E) \sim E^{-2.0}$, which is consistent with published results [15]. Theory predicts critical scaling in this model to occur when the maximum number of permitted rearrangements $n_{\max}$ of each fiber is large, and theoretical calculations of the values of the scaling exponents have been found to agree very well with experimental observations of fluctuations in a compressed granular system [15].

An example showing the response of the inverse Fiber Bundle Model to a dynamically variable applied stress (load profile recorded from a human footstep), is shown in Figure 11. Although the behavior observed is plausibly realistic, with most fracture energy produced during initial loading (heel strike) and in stress buildup prior to unloading (toe off), a more realistic response would be obtained if the spatially distributed nature of foot-ground contact were accounted for.

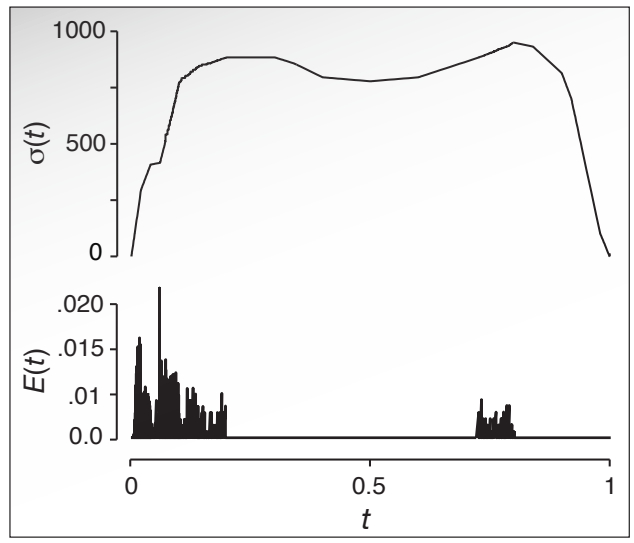

Fig. 11. The response of a granular medium, represented by a bundle of 2000 iFBM fibers, to a dynamic load, consisting of recorded data from a human footstep. Shown are the applied load $\sigma(t)$, and the energy $E(t)$ computed in windows of duration $\Delta t = 0.005$.

Distributed and spatially varying media This paper has so far treated interactions with heterogeneous materials with material properties that are constant, in a statistical sense, within the simulated volume. This work could also be extended to address to interactive simulation of fracture processes that vary in space, or that transfer load preferentially to nearby fibers [19], as in large volume of distributed granular material (Fig. 12). This is facilitated by the mean damage approximation. In a distributed setting, the averaged nonlinear strain response (Eq. (23) for the inverse Fiber Bundle Model) can be obtained from a homogenized continuum mechanics model of the constitutive behavior of the distributed medium, simulated using finite element, elastic mesh, or point cloud methods. Using our model, fracture processes can be simulated by associating independent instances $\xi_k(t)$ of the fracture process effective volume elements (at points $\mathbf{x}_k$) defined by finite elements or by point based radial basis functions $\Phi_i(\mathbf{x})$. Conditions for local fracture can then be obtained from a measure of maximal strain obtained from the strain tensor ε, similar to criteria used to nucleate and grow cracks in continuous media for computer graphics rendering [39, 36, 37]. Since the constitutive behavior is smooth, it can be integrated at a lower sample rates than those used to render fracture events.

5 Interactive Multimodal Rendering of Heterogeneous Fracture

Interactive simulation of failure processes in quasi-brittle, heterogeneous materials is of interest for scientific visualization or immersive virtual reality. By virtue of the stochastic formulation reviewed above,

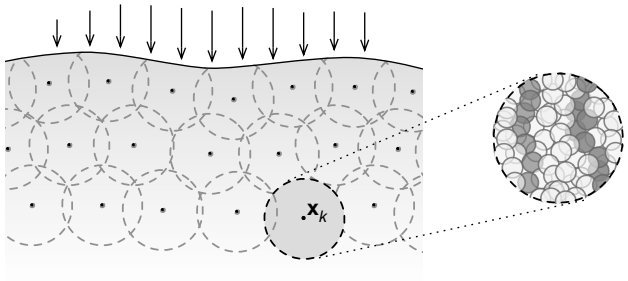

Fig. 12. Rendering high-frequency failure processes in distributed media at interactive rates is facilitated by the separation they provide between the slower, homogenized volumetric response and the rapid fluctuations, which can be represented through local, stress-driven fracture processes associated with points $\mathbf{x}_k$.

it was possible to implement the algorithms efficiently, at audio sampling rate ($f_s = 48$ kHz). This made it possible to reproduce stress fluctuations accompanying fracture evolution across the entire vibrotactile and audible bandwidths (Fig. 13). Figure 15 shows a still frame from an interactive simulation, with control and force feedback mediated via a haptic interface (Falcon, Novint Inc., with libnifalcon open source drivers), and with concurrent auditory feedback. The simulation runs in real time at high sampling rates (dynamics and audio: 48 kHz, haptic control loop: 1 kHz).

A variable stress $\sigma(t)$ (either simulated or acquired via instrumentation) is provided as a real-time input to the dynamics, resulting in a time-varying strain $x(t)$, computed as the solution of Equation (1). Fracture events occur as described in Eq. (11)-(12). Each event evokes a sequence of transient failures with energies $E = \Delta N k_F x(t)^2$, where ΔN is the number of fibers that fail in a given time-step.

In the implementation, discretization of the dynamics was performed via Laplace transformation of the ordinary differential equations, followed by the bilinear transform mapping from the s- to the z-plane. This allows the constitutive response of the system to be implemented via low-order infinite impulse response (IIR) discrete time filters. This explicit integration method provides a reasonable accuracy-performance tradeoff at high (audio bandwidth) sampling rates [44], far better than is achieved with a finite-difference discretization of comparable order. At low frequencies, both finite-difference and bilinear transform discretizations produce essentially equivalent results.

The fracture algorithm requires minimal computation. When fracture events are sparse, most computation time is spent on the integration; for model M, the stress-strain dynamics may be implemented as a second order IIR filter requiring five multiply-accumulate operations per sample period. As the density of fracture events per sample period increases, computation time is increasingly spent updating the breaking threshold ξ after each failure, which requires calculating the inverse fiber strength CDF $P^{-1}(\cdot)$. However, by interpolating values stored in a function table or by precomputing sampled thresholds, this cost is reduced to a small, constant number of operations per fracture event.

Random Modal Filter Model of Acoustic Transfer The quality of mechanical vibrations or acoustic emissions from fracture processes are strongly determined by the transfer properties of the medium. The latter strongly influence the perception of these acoustic events, especially for natural materials such as wood [11, 21]. Thus, the rendering algorithm includes a linear filter model of acoustic transfer in the medium (Fig. 14). It is represented by a modal resonant filter with impulse response [7]

$$h(t) = \sum_{i=1}^{M} A_i e^{-b_i t} \sin(2\pi f_i t). \tag{26}$$

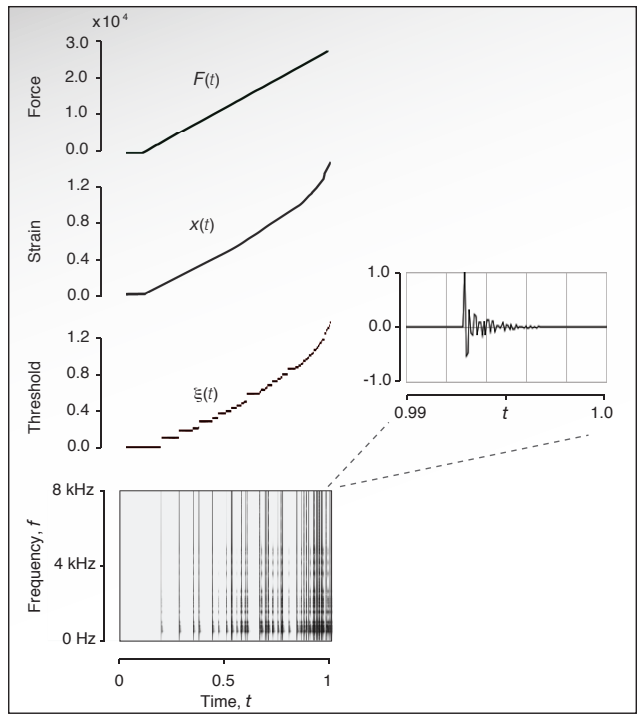

Fig. 13. Representative data from a real-time implementation of Fiber Bundle Model M. Data shown corresponds to a model with 350 fibers. Acoustic transfer is simulated by a resonant filter with $N = 10$ modes. Left column, Top to Bottom: Force input $F(t)$, strain $x(t)$, threshold $\xi(t)$, and time-frequency spectrogram of acoustic energy of fracture. Right: Fracture event waveform.

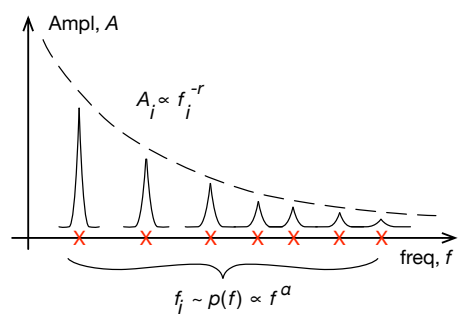

Fig. 14. The magnitude frequency response of a random modal filter model used to model acoustic transfer in the simulated medium captures the physical phenomena of geometric growth of mode density and damping-dependent decrease in amplitude with frequency, using just two key parameters.

Although the resonant filter parameters could, in principle, be precomputed by modeling the material geometry and constitution, a simpler approach is adopted here. Resonant frequencies f_i are selected to be randomly distributed as $p(f) \propto f^{\alpha}$, where the parameter α controls the rate of growth of mode density with frequency. In real materials, this is related to the geometry, dimension, and wave velocity of the propagating medium. Decay factors b_i describe the filter bandwidth, which is related to the intrinsic damping in the material. The amplitudes A_i are chosen to provide a decaying spectrum envelope with $A_i = A_0 f_i^{-r}$. This rate of amplitude decrease with frequency corresponds to a decay of $6r$ dB/octave [44], modeling frequency-dependent damping in acoustic propagation. By choosing the number

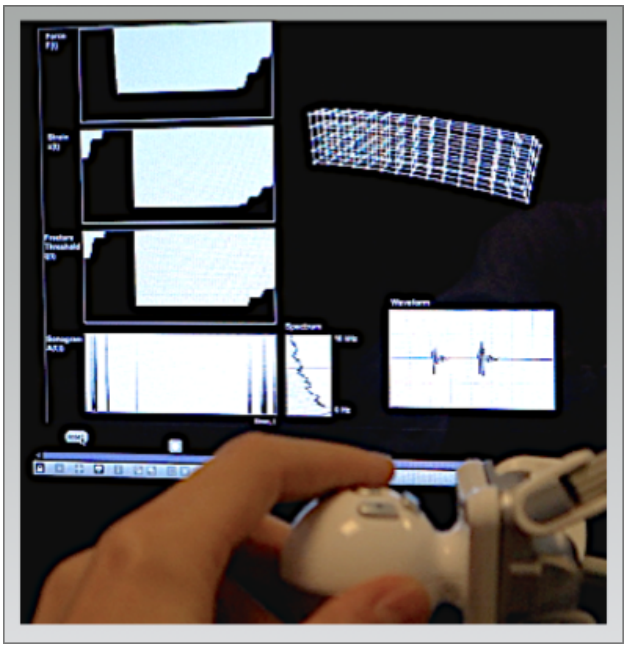

Fig. 15. Interactive haptic and auditory rendering of fracture in a wood beam, using the physical model presented here. Data shown corresponds to a model with 700 fibers. Acoustic transfer is simulated by a resonant filter with $N = 10$ modes. The mesh shown is a mass-spring model to which we apply strain computed by the model for visualization purposes. The beam bending in the mesh-spring model is driven by the lumped parameter stochastic fracture model, for the purpose of visualizing strain.

N_m of modes, their decay rate r with frequency, and their distribution α appropriately, the acoustic response can be shaped to qualitatively resemble the material of interest (e.g., wood, stone; see Supplementary material).

6 Conclusions

This paper presented algorithms for simulating failure in quasi-brittle heterogeneous materials, such as natural fiber composites and granular materials, based on recently developed formulations of two well-established lattice physical models: the Fiber Bundle Model and Inverse Fiber Bundle Model. The constructions involved accurately reproduce the deterministic and stochastic response of the exact algorithms, in agreement with known physics. In short, these algorithms can accurately reproduce the most salient features of rapid fracture in fiber composite and granular materials. The main purpose of introducing these constructions here is that they facilitate the efficient simulation of these complex processes for the first time, by eliminating the need to dynamically integrate large numbers of spatial degrees of freedom, and by homogenizing the constitutive (stress-strain) behavior. The latter has the further effect of isolating the fast varying dynamical degrees of freedom, preventing them from contributing transient fluctuations to the dynamical state, and reducing the computation required for integrating the stress-strain dynamics to a small, constant number of operations per sample period.

The method applied here considers failure due to a load applied along a single dimension, which could be viewed as a limitation. For fiber composite materials (such as wood), stresses with arbitrary directions can readily be accommodated in the model presented here by decomposing applied stress according to the fiber geometry. Granular materials rearrange load bearing structures in more complicated ways as the direction of applied stress is varied. As such, more work is needed in order to adapt the method presented here to such cases.

The model presented here is efficient enough to simulate stress fluctuations in hundreds to hundreds of thousands of distributed fibers in real-time. This could aid a wide range of applications in virtual reality simulation of natural environments, and could enable others in scientific simulation and in interactive visualization.

References

[1] F. Adjémian and P. Evesque. Different regimes of stick-slip in granular matter: from quasi- periodicity to randomness. *EGS XXVII General Assembly, Nice, 21-26 April 2002*, 2002.

[2] M. Alava, P. Nukala, and S. Zapperi. Statistical models of fracture. *Advances in Physics*, 55(3):349–476, 2006.

[3] Y. Visell and G. Millet. Fracture in disordered heterogeneous materials as a stochastic process. *arXiv:1408.530.3 (cond-mat.stat.mech)*, 2014.

[4] A. Baldassarri, F. Dalton, A. Petri, S. Zapperi, G. Pontuale, and L. Pietronero. Brownian forces in sheared granular matter. *Physical review letters*, 96(11):118002, 2006.

[5] N. Bell, Y. Yu, and P. Mucha. Particle-based simulation of granular materials. In *Proceedings of the 2005 ACM SIGGRAPH/Eurographics symposium on Computer animation*, page 86. ACM, 2005.

[6] R. Chudoba, M. Vořechovskỳ, and M. Konrad. Stochastic modeling of multi-filament yarns. i. random properties within the cross-section and size effect. *International Journal of Solids and Structures*, 43(3):413–434, 2006.

[7] P. Cook. *Real Sound Synthesis for Interactive Applications*. AK Peters, Ltd., 2002.

[8] F. Dalton, F. Farrelly, A. Petri, L. Pietronero, L. Pitolli, and G. Pontuale. Shear stress fluctuations in the granular liquid and solid phases. *Physical review letters*, 95(13):138001, 2005.

[9] L. Devroye. *Non-Uniform Random Variate Generation*. Springer Verlag, 1986.

[10] G. Dill-Langer, R. C. Hidalgo, F. Kun, Y. Moreno, S. Aicher, and H. Herrmann. Size dependency of tension strength in natural fiber composites. *Physica A: Statistical Mechanics and its Applications*, 325(3):547–560, 2003.

[11] B. L. Giordano and S. McAdams. Material identification of real impact sounds: Effects of size variation in steel, glass, wood, and plexiglass plates. *The Journal of the Acoustical Society of America*, 119(2):1171–1181, 2006.

[12] L. Glondu, M. Marchal, and G. Dumont. Real-time simulation of brittle fracture using modal analysis. *Visualization and Computer Graphics, IEEE Transactions on*, 19(2):201–209, 2013.

[13] A. Hansen and P. Hemmer. Burst avalanches in bundles of fibers: Local versus global load-sharing. *Physics Letters A*, 184(6):394–396, 1994.

[14] H. Herrmann and S. Roux. *Statistical models for the fracture of disordered media*. North Holland, 1990.

[15] R. Hidalgo, C. Grosse, F. Kun, H. Reinhardt, and H. Herrmann. Evolution of percolating force chains in compressed granular media. *Physical review letters*, 89(20):205501, 2002.

[16] R. Hidalgo, F. Kun, and H. Herrmann. Bursts in a fiber bundle model with continuous damage. *Physical Review E*, 64(6):66122, 2001.

[17] R. Hidalgo, F. Kun, and H. Herrmann. Slow relaxation of fiber composites, variable range of interaction approach. *Physica A: Statistical Mechanics and its Applications*, 347:402–410, 2005.

[18] R. C. Hidalgo, H. J. Herrmann, F. Kun, and E. Partelli. Force chains in granular packings. In F. Mallamace and H. Stanley, editors, *The Physics of Complex Systems*. IOS Press, Amsterdam, 2004.

[19] R. C. Hidalgo, Y. Moreno, F. Kun, and H. J. Herrmann. Fracture model with variable range of interaction. *Physical review E*, 65(4):046148, 2002.

[20] K. Hirota, Y. Tanoue, and T. Kaneko. Generation of crack patterns with a physical model. *The Visual Computer*, 14(3):126–137, 1998.

[21] R. L. Klatzky, D. K. Pai, and E. P. Krotkov. Perception of material from contact sounds. *Presence: Teleoperators and Virtual Environments*, 9(4):399–410, 2000.

[22] M. Kloster, A. Hansen, and P. C. Hemmer. Burst avalanches in solvable models of fibrous materials. *Physical Review E*, 56(3):2615, 1997.

[23] R. Koerner, W. McCabe, and A. Lord Jr. Acoustic emission behavior and monitoring of soils. In *Acoustic emissions in geotechnical engineering practice: a symposium*, page 93. ASTM International, 1981.

[24] F. Kun, S. Zapperi, and H. J. Herrmann. Damage in fiber bundle models. *The European Physical Journal B-Condensed Matter and Complex Systems*, 17(2):269–279, 2000.

[25] T. Lenaerts, B. Adams, and P. Dutré. Porous flow in particle-based fluid simulations. *ACM Transactions on Graphics (TOG)*, 27(3):49, 2008.

[26] M. Lin and M. Otaduy. *Haptic rendering: foundations, algorithms, and applications*. AK Peters Ltd, 2008.

[27] N. Liu, X. He, S. Li, and G. Wang. Meshless simulation of brittle fracture. *Computer Animation and Virtual Worlds*, 22(2-3):115–124, 2011.

[28] K. Loades, A. Bengough, M. Bransby, and P. Hallett. Planting density influence on fibrous root reinforcement of soils. *Ecological Engineering*, 36(3):276–284, 2010.

[29] S. Mérillou and D. Ghazanfarpour. A survey of aging and weathering phenomena in computer graphics. *Computers & Graphics*, 32(2):159–174, 2008.

[30] G. Michlmayr, D. Cohen, and D. Or. Sources and characteristics of acoustic emissions from mechanically stressed geologic granular media—a review. *Earth-Science Reviews*, 112(3):97–114, 2012.

[31] L. Mishnaevsky Jr and P. Brøndsted. Micromechanical modeling of damage and fracture of unidirectional fiber reinforced composites: A review. *Computational Materials Science*, 44(4):1351–1359, 2009.

[32] M. Müller, L. McMillan, J. Dorsey, and R. Jagnow. *Real-time simulation of deformation and fracture of stiff materials*. Springer, 2001.

[33] S. Nasuno, A. Kudrolli, A. Bak, and J. Gollub. Time-resolved studies of stick-slip friction in sheared granular layers. *Physical Review E*, 58(2):2161–2171, 1998.

[34] S. Nasuno, A. Kudrolli, and J. Gollub. Friction in granular layers: hysteresis and precursors. *Physical Review Letters*, 79(5):949–952, 1997.

[35] A. Norton, G. Turk, B. Bacon, J. Gerth, and P. Sweeney. Animation of fracture by physical modeling. *The Visual Computer*, 7(4):210–219, 1991.

[36] J. O'Brien and J. Hodgins. Graphical modeling and animation of brittle fracture. In *Proc of the 26th annual conference on Computer graphics and interactive techniques*, pages 137–146. ACM Press/Addison-Wesley Publishing Co. New York, NY, USA, 1999.

[37] E. Parker and J. O'Brien. Real-time deformation and fracture in a game environment. In *Proceedings of the 2009 ACM SIGGRAPH/Eurographics Symposium on Computer Animation*, pages 165–175. ACM, 2009.

[38] E. G. Parker and J. F. O'Brien. Real-time deformation and fracture in a game environment. In *Proceedings of the 2009 ACM SIGGRAPH/Eurographics Symposium on Computer Animation*, pages 165–175. ACM, 2009.

[39] M. Pauly, R. Keiser, B. Adams, P. Dutré, M. Gross, and L. Guibas. Meshless animation of fracturing solids. *Proceedings of the 2005 ACM SIGGRAPH/Eurographics Symposium on Computer Animation*, 24(3):957–964, 2005.

[40] S. Pradhan, A. Hansen, and B. Chakrabarti. Failure processes in elastic fiber bundles. *Reviews of Modern Physics*, 82(1):499–555, 2010.

[41] N. M. Pugno, F. Bosia, and T. Abdalrahman. Hierarchical fiber bundle model to investigate the complex architectures of biological materials. *Physical Review E*, 85(1):011903, 2012.

[42] I. Reiweger, J. Schweizer, J. Dual, and H. Herrmann. Modelling snow failure with a fibre bundle model. *Journal of Glaciology*, 55(194):997–1002, 2009.

[43] A. Rinaldi. Statistical model with two order parameters for ductile and soft fiber bundles in nanoscience and biomaterials. *Physical Review E*, 83(4):046126, 2011.

[44] J. Smith. *Physical audio signal processing*. J. O. Smith, 2004.

[45] J. Smith, A. Witkin, and D. Baraff. Fast and controllable simulation of the shattering of brittle objects. In *Computer Graphics Forum*, volume 20, pages 81–91. Wiley Online Library, 2001.

[46] S. M. Sutherland. *Fibre based modeling of wood dynamics and fracture*. PhD thesis, University of British Columbia, 2012.

[47] D. Terzopoulos and K. Fleischer. Deformable models. *The visual computer*, 4(6):306–331, 1988.

[48] W. Weibull. A statistical distribution function of wide applicability. *Journal of applied mechanics*, 1951.

[49] C. Zheng and D. L. James. Rigid-body fracture sound with precomputed soundbanks. *ACM Transactions on Graphics (TOG)*, 29(4):69, 2010.

[50] Y. Zhu and R. Bridson. Animating sand as a fluid. In *ACM SIGGRAPH 2005 Papers*, page 972. ACM, 2005.